Supporting Information

MANUSCRIPT TITLE: A field, laboratory and modeling study of reactive transport of groundwater arsenic in a coastal aquifer

AUTHOR NAMES: Hun Bok Jung[1], Matthew A. Charette[2], Yan Zheng[1, 3]

AUTHOR ADDRESSES: [1]School of Earth and Environmental Sciences, Queens College and the Graduate School and University Center, The City University of New York, Flushing, NY 11367 United States; [2]Department of Marine Chemistry and Geochemistry, Woods Hole Oceanographic Institution, Woods Hole, MA 02543 United States; [3]Lamont-Doherty Earth Observatory of Columbia University, Palisades, NY 10964 United States

We describe sampling and analysis methods (sections 1, 2 and 3), hydrologic and chemical settings and parameters used in the multi-component reactive transport model PHT3D to simulate As transport at the Waquiot Bay coastal aquifer (section 4). Additional modeling results of PHT3D that illustrate pH and As speciation in simulations and sensitivity tests are reported (section 5). PHT3D is also used to estimate Kd from an As(V) injection experiment performed in the Cape Cod aquifer (Höhn et al., 2006) studied by USGS (section 6).

1. Water sampling and Analysis of As and Fe

Pore water samples were collected using a stainless steel drive point piezometer system ("Retract-A-Tip", AMS Inc) (Charette and Allen, 2006). Samples were obtained between approximately 1 m and 7 m at PZ10, 1 m and 4 m at PZ6, and 1 and 8 m depth at PZ3 with 0.3-0.45 m depth resolution for the fresh groundwater portion and 0.6 m depth resolution for the saline groundwater portion (Table S1). Groundwater samples were drawn to the surface through acid-cleansed nylon tubing using a peristaltic pump at a flow rate of 500 ml min^{-1}. After a minimum 3-fold flushing the tubing volume and stabilization of the reading of the oxidation reduction potential (ORP), pH, dissolved oxygen, and temperature that were measured using a YSI 600XLM in a flow through cell (YSI Inc), samples filtered through an inline 0.45 μm Pall AquaPrep 600 filter were collected in 20 mL acid-cleaned high-density polyethylene (HDPE) liquid scintillation vials (Wheaton Science). Immediately after sample collection without acidification in the field, dissolved Fe(II) was measured by a ferrozine colorimetry method (Stookey, 1970). As(III) was measured by differential pulse cathodic stripping voltammetry (DPCSV) with a detection limit of ~0.2 μg L^{-1} (He et al., 2004). An Eco Chemie μAutolab voltammetric apparatus (Brinkmann Instruments, Westbury, NY) equipped with a Metrohm 663VA electrode stand and controlled by a laptop computer running ECO Chemie GPES 4.95 software. Then, samples were acidified to 1% HCl (Optima, Fisher). Dissolved As and Fe concentrations were determined by HR ICP-MS that has a detection limit of 0.1 μg L^{-1} for As and 0.4 μg L^{-1} for Fe (Cheng et al., 2004).

Bay water sample was collected in a 20mL scintillation vial about 5 m away from the shoreline, and was acidified to 1% HCl after filtration through a 0.45 μm syringe filter.

Total As in the bay water was determined by DPCSV after reducing all inorganic As(III+V) to As(III) with 20mM L-cysteine (He et al., 2007).

2. *Sediment sampling and Analysis of As and Fe*

Sediment samples were placed in an anaerobic glove bag filled with ultra pure N_2 gas in the field immediately after sample collection (Table S2). Within hours of sample collection, 5 to 10 g of samples with a 0.3 m depth resolution were leached with 7 mL of 1.2N HCl in 15 mL centrifuge tube (BD Falcon) at 80 ℃ for 1hr to liberate elements associated with amorphous and labile crystalline Fe oxyhydroxides phases (Horneman et al, 2004). Total Fe and Fe(II) in the leachates were determined by a colorimetric technique using ferrozine solution in the field (Stookey, 1970; Horneman et al., 2004). To evaluate As sorbed on the sediment surface, sediments were extracted by a N_2-purged 1M sodium phosphate (Fisher) solution containing 0.1 M ascorbic acid for 36hrs in 15mL crimp sealed amber vials under anaerobic condition. Concentrations of As(III) in the phosphate extract were determined by DPCSV in the field, while total As concentrations were determined by HR ICP-MS in the laboratory (Jung and Zheng, 2006). The sediment HCl leachates were also analyzed by HR ICP-MS similarly for As.

3. *Analytical Methods for dissolved and sedimentary As*

For DPCSV analysis of As(III), stock standard solution of 1000 mg L^{-1} As(III) was prepared by dissolving sodium *m*-arsenite ($NaAsO_2$) in nano-pure water (>18 MΩ) containing 1 g L^{-1} ascorbic acid, which was added to prevent oxidation of arsenite (He et al., 2004). Concentration of dissolved As(III) in the filtered and acidified supernatant was determined by DPCSV while total dissolved As by HR ICP-MS (Cheng et al., 2004). Sediment samples after equilibration with As(III) for adsorption experiment were sequentially extracted by 1M sodium phosphate for 36 hrs and then by 1.2N hot HCl for 1 hr. The As(III) in the phosphate leachate was determined by DPCSV. Total As in both the phosphate and HCl leachates, was determined by HR ICP-MS.

4. *Detailed hydrologic and chemical settings for PHT3D modeling*

The aquifer bulk density was set to 1.875 g cm^{-3} based on the aquifer porosity of 0.35 and the density of dry sand of 2.65 g cm^{-3} (Michael et al., 2005). For the upland side, constant head boundary condition was selected, while for the Waquoit Bay side, river boundary condition was selected to allow the fresh groundwater to discharge towards the bay, and all other sides were no flow boundaries. At the river boundary, the thickness of the riverbed, the hydraulic conductivity of the riverbed, and the width of river were assigned to be 0.5 m, 8.64 m d^{-1} and 10 m, respectively, which is consistent with Michael et al (2005) showing that hydraulic conductivity is similar for aquifer sediment and bay sediment, and most fresh groundwater discharges within ~10 m distance from the shore. Shore normal freshwater flux of 0.484 m^3 d^{-1} simulated by PHT3D is within the range of 0.142~1.558 m^3 d^{-1} of fresh water flux measured by seepage meters along 60-150 m of shoreline (Michael et al., 2003), and comparable to the hydrogeologic estimate of 1.234 m^3 d^{-1} in front of the low lying areas along 210 m of shoreline, which includes our study site (Mulligan and Charette, 2006).

To simulate the transport of As along the flow path, the fresh groundwater enters the model from the upland boundary and flow towards the bayside boundary. The composition of upland groundwater enters the boundary is simplified to capture the conditions commonly observed, with 500 μM of Na and Cl, 300 μM of Ca and 600 μM of HCO$_3$ (Stollenwerk, 1995; Höhn et al., 2006). Three 2-m intervals are specified, with an anoxic zone (pH = 7) and two oxic zones with DO of 3 mg L^{-1} above and below (pH = 6). The oxic groundwater contains no dissolved Fe(II) and As(III). The reducing groundwater contains 5.6 mg L^{-1} of Fe(II) and 15 μg L^{-1} of As(III). The recharging fresh water (pH = 6) with 10 mg L^{-1} of O$_2$ contains 500 μM of Na and Cl for charge balance. The recharging saline water (pH= 8) near shore has 10 mg L^{-1} of O$_2$, and 5 mM of Na and Cl.

For the parametric Kd-based reactions in PHT3D, four Kd values of 25, 60, 90 and 120 L kg^{-1} representing 4 horizontal redox zones along the flow path towards the bay were parameterized. The Kd values were estimated based on the sedimentary Fe(II)/Fe of 0.8, 0.6, 0.4 and 0.2 that capture the increasing average percentage of Fe(III) in the sediment cores toward the bay using an empirical relationship derived from batch adsorption experiment:

Kd (L kg^{-1}) = -164 × Sed Fe(II)/Fe + 155 (R^2 = 0.999)

To establish this empirical relationship, three Kd values were first calculated from three experimentally determined Langmuir isotherms (Fig. 2) at equilibrium with dissolved As concentration measured at each field site. Then a linear regression was performed.

For the SCM based reactions in PHT3D, surface site density of 1.1, 1.5, 3.0, and 4.0 µM g^{-1} representing 4 horizontal redox zones along the flow path towards the bay were parameterized. These values were chosen in part due to the SCM model fit to sorption experimental data generated reasonable results using a set of values similar to these (Fig. 2). In addition, previous studies of surface properties of reducing sediment from the Cape Cod aquifer extensively evaluated by USGS were considered. Surface site density for unsaturated aquifer sediment in USGS research site on Cape Cod is reported to be 1.1~1.2 µM g^{-1} by potentiometric titration of sediment with H$^+$ (Stollenwerk, 1995) and by calculation based on specific surface area (Kent et al., 1995). Because the selectively leached poorly crystalline hydrous Fe oxide (95 mg/kg Fe) in the aquifer sediment from USGS site (Kent et al., 1995) is comparable to the average HCl leachable Fe oxide concentration (80 mg/kg FeIII) in the reducing sediment at our site, the value of 1.1 µM g^{-1} is adopted to represent reducing sediment here. The surface site density and conditional equilibrium constants, the same as the diffuse layer model (DLM) of ferrihydrite (Dzombak and Morel, 1990), were defined in a subcode (postfix.phrq) for surface complexation reactions in PHT3D.

5. Simulation by PHT3D and sensitivity test

_pH._ The simulated pH captures both the vertical and horizontal gradients in the field data. Like dissolved Fe (Fig. 3), simulated pH quickly reaches steady state in ~ 20 years with values of ~ 6.7 in the top and bottom layers. Along the plume, pH averages ~7.5, and is ~8.1, ~7.8, and ~6.7 at PZ10, PZ6, and PZ3, respectively. The simulated pH is comparable to the field observation at PZ6 and PZ3, but is higher than field observed value of ~7.2 at PZ10. Although the pH in the center of plume at PZ10 is overpredicted, it is not likely to affect the transport of dissolved As because adsorption of As(III) by Fe oxides is not sensitive to pH when pH is 6-9 (Dixit and Hering, 2003).

As speciation. In the PHT3D simulation, the speciation of dissolved As is determined by oxidation of As(III) by dissolved oxygen. Therefore, the simulated As speciation in the center of reducing plume, is nearly 100% As(III) at PZ10 and PZ6 due to absence of dissolved oxygen, and is almost ~100% As(V) at PZ3 due to abundant oxygen supplied from the surface. The field data show dominance of As(V) at PZ6. This may be attributed to absence of Mn oxide in the model, which could oxidize dissolved As(III) at PZ6 in the field (Amirbahman et al., 2006). Nevertheless, this inconsistency in As speciation would cause a minor effect on the As transport because As(III) and As(V) have a similar affinity for Fe oxides at near-neutral pH conditions (Dixit and Hering, 2003).

Sensitivity test. PHT3D was run with three hydraulic gradients, 0.004, 0.009 and 0.020, and the effect on Fe-oxides precipitation was tested. The values were chosen because hydraulic gradient across the head of Waquoit Bay varies from 0.004 to 0.022 at high tide and from 0.002 to 0.015 at low tide (Mulligan and Charette, 2006).

PHT3D was also run with variable recharge rate scenarios to test the effect on Fe-oxides precipitation. The default setting reported in the text is as follows. A recharge rate for Zones 1 and 2 is 0.001 m d^{-1}, representing the average recharge rate to the aquifer (Michael et al., 2005), 0.005 m d^{-1} for Zone 3, and 0.01 and 0.05 m d^{-1} in first and second half of Zone 4 (Fig. 3) to reflect the tidal infiltration and near-shore circulation due to tides and waves. To examine the model sensitivity to tide or waves near shore, the recharge rate was varied by a factor 4 in Zones 3 and 4, increasing the recharge rate from 0.002 to 0.005 and 0.010 m d^{-1} in Zone 3, while from 0.005 to 0.01 and 0.02 m d^{-1} in the first half of Zone 4 and from 0.025 to 0.05 and 0.1 m d^{-1} in the second half of Zone 4.

As the result, simulated Fe oxide precipitation is not sensitive to a factor of 4~5 variation of hydraulic gradient and recharge rate showing the variation of < 10%. Furthermore, simulated As concentration is not affected by simulated Fe oxide precipitation because As adsorption in PHT3D simulation is controlled by spatially assigned surface site densities using a subcode (postfix.phrq).

6. Simulation of an As(V) injection experiment by PHT3D

To further establish that the reducing sediment from the USGS study site in the upgradient region of the Cape Cod aquifer has surface properties similar to those in the

reducing zones at Waquiot Bay, a Kd-based PHT3D was used to simulate the migration of an injected arsenate plume. Höhn et al (2006) injected groundwater pumped from the suboxic zone amended with 6.7 μM As(V) continuously at a rate of ~25 L h^{-1} into the anoxic iron reducing zone of the aquifer for 4 weeks. The injected As(V) plume was monitored at 10 wells down gradient for 104 days. Injected As(V) was observed to be reduced to As(III) after approximately 1 week after terminating the injection, and the plume migrated ~4.5 m down gradient at the end of the observational period. Applying the same hydrological and geochemical parameters reported in Höhn et al (2006), the observed migration of As(III) and As(V) plumes can be simulated using PHT3D (Fig. S3) when a Kd value of 4 L kg^{-1} is used for a final median equilibrated [As] of ~75 μg L^{-1} in the plume. This is equivalent to a Kd value of 30 for an equilibrated [As] of 10 μg L^{-1}, assuming the same Langmuir sorption isotherm for the reducing sediments as dark gray sediment at PZ7 (Table 1, Fig. S4). Unlike Höhn et al (2006)'s experiment showing gradual reduction of As(V) to As(III) in the plume after termination of As(V) injection and reestablishment of reducing condition, resulting in ~30% of dissolved As in the form of As(V) in ~100 days, PHT3D modeling simulated more rapid and complete reduction of As(V) to As(III) in the plume immediately after As(V) injection was terminated, resulting in > 99% of dissolved As in the form of As(III) in ~100 days.

References

Amirbahman, A.; Kent, D.B.; Curtis, G.P.; Davis, J.A. Kinetics of sorption and abiotic oxidation of arsenic(III) by aquifer materials. Geochim. Cosmochim. Acta 2006, 70, 533-547.

Baes, C.F.; Sharp, R.D. A Proposal for Estimation of Soil Leaching and Leaching Constants for Use in Assessment Models. J. Environ. Qual. 1983, 12, 17–28.

BGS & DPHE. In: Kinniburgh, D.G., Smedley, P.L. (Eds.), Arsenic Contamination of Groundwater in Bangladesh, British Geological Survey WC/00/19, Keyworth, UK, 2001.

Charette, M.A.; Allen, M.C. Precision Ground Water Sampling in Coastal Aquifers Using a Direct-Push, Shielded-Screen Well-Point System. Ground Water Monitoring & Remediation 2006, 26, 87-93.

Cheng, Z.; Zheng, Y.; Mortlock, R.; van Geen, A. Rapid multi-element analysis of groundwater by high-resolution inductively coupled plasma mass spectrometry. Anal. Bioanal. Chem. 2004, 379, 512-528.

DPHE/BGS/MML. Groundwater studies for arsenic contamination in Bangladesh, Main Report, Phase 1: Rapid investigation phase. Department of Public Health Engineering (DPHE), Government of Bangladesh, British Geological Survey, UK and Mott MacDonald Ltd., Dhaka, Bangladesh, 1999.

Dixit, S.; Hering, J.G. Comparison of Arsenic (V) and Arsenic (III) Sorption onto Iron Oxide Minerals: Implication for Arsenic Mobility. Environ. Sci. Technol. 2003, 37, 4182-4189.

Dzombak, D.A.; Morel, F.M.M. Surface Complexation Modeling: Hydrous Ferric Oxide. Wiley-Interscience, New York, 1990.

He, Y.; Zheng, Y.; Locke, D.C. Cathodic stripping voltammetric analysis of arsenic species in environmental water samples. Microchem. J. 2007, 85, 265-269.

He, Y.; Zheng, Y.; Ramnaraine, M.; Locke, D.C. Differential pulse cathodic stripping voltammetric speciation of trace level inorganic arsenic compounds in natural water samples. Anal. Chim. Acta 2004, 511, 55-61.

Höhn R.; Isenbeck-Schröter, M.; Kent, D.B.; Davis, J.A.; Jakobsen, R.; Jann, S.; Niedan, V.; Scholz, C.; Stadler, S.; Tretner, A. Tracer test with As(V) under variable redox

conditions controlling arsenic transport in the presence of elevated ferrous iron concentrations. J. Contam. Hydrol. 2006, 88, 36-54.

Horneman, A.; van Geen, A.; Kent, D.V.; Mathe, P.E.; Zheng, Y.; Dhar, R.K.; O'Connell, S.; Hoque, M.A.; Aziz, Z.; Shamsudduha, M.; Seddique, A.A.; Ahmed. K.M. Decoupling of As and Fe release to Bangladesh groundwater under reducing conditions. Part 1: Evidence from sediment profiles. Geochim. Cosmochim. Acta 2004, 68, 3459-3473

Kent, D.B.; Davis, J.A; Anderson, L.C.D.; Rea, B.A. Transport of chromium and selenium in a pristine sand and gravel aquifer: Role of adsorption processes. Wat. Resour. Res. 1995, 31, 1041-1050.

Kuhlmeier, P.D. Sorption and desorption of arsenic from sandy soils: column studies. J. Soil Contam. 1997, 6, 21–36.

Jung, H.B.; Zheng, Y. Enhanced recovery of arsenite sorbed onto synthetic oxides by L-ascorbic acid addition to phosphate solution: calibrating a sequential leaching method for the speciation analysis of arsenic in natural samples. Wat. Res. 2006, 40, 2168-2180.

Manning, B.A.; Goldberg, S. Arsenic(III) and arsenic(V) adsorption on three California soils. Soil Sci. 1997, 162, 886-895.

Michael, H.A.; Lubetsky, J.S.; Harvey, C.F. Characterizing submarine groundwater discharge: a seepage meter study in Waquoit Bay, Massachusetts. Geophys. Res. Lett. 2003, 30, doi:10.1029/2002GL016000.

Michael, H.; Mulligan, A.; Harvey, C. F. Seasonal Water Exchange between Aquifers and the Coastal Ocean. Nature 2005, 436, 1145-1149.

Mulligan, A.E.; Charette, M.A. Intercomparison of submarine groundwater discharge estimates from a sandy unconfined aquifer. J. Hydrol. 2006, 327, 411-425.

Prommer, C.; Barry, D.A.; Zheng, C. MODFLOW/MT3DMS-Based Reactive Multicomponent Transport Modeling. Ground Water 2003, 41, 247-257.

Stollenwerk, K.G. Modeling the effects of variable groundwater chemistry on adsorption of molybdate. Wat. Resour. Res. 1995, 31, 347-357.

Stookey, L.L. Ferrozine - A new spectrophotometric reagent for iron. Anal. Chem. 1970, 42, 779-781.

Sullivan, K.A.; Aller, R.C. Diagenetic cycling of arsenic in Amazon shelf sediments. Geochim. Cosmochim. Acta 1996, 60, 1465-1477.

van Geen A.; Zheng Y.; Goodbred S.; Horneman A.; Aziz Z.; Cheng Z.; Stute M.; Mailloux B.; Weinman B.; Hoque M.A.; Seddique A.A.; Hossain M.S.; Chowdhury S.H.; Ahmed K.M. Flushing history as a hydrogeological control on the regional distribution of arsenic in shallow groundwater of the Bengal Basin. Environ. Sci. Technol. 2008, 42, 2283-2288.

Williams, L.E.; Barnett, M.O.; Kramer, T.A.; Melville, J.G. Adsorption and Transport of Arsenic(V) in Experimental Subsurface Systems. J. Environ. Qual. 2003, 32, 841-850.

Table S1. Pore Water Chemical Composition Data

Piezometer No	Sample No	Depth	pH	Eh	Salinity	Fe	FeII	As	AsIII	P	S	Mn
		m		mV		mg/L	mg/L	ug/L	ug/L	mg/L	mg/L	ug/L
PZ10	WB7-1	0.9	5.62	180	0.14	0.027	nd	<0.1	<0.2	0.02	5.64	17
	WB7-2	1.35	5.84	372	0.17	0.028	nd	<0.1	<0.2	0.02	5.49	20
	WB7-3	1.8	5.83	400	0.38	0.038	nd	0.1	<0.2	0.04	4.60	74
	WB7-4	2.25	6.9	292	0.48	0.061	0.028	1.0	nd	0.14	14.04	28
	WB7-5	2.7	7.18	154	0.33	0.461	0.434	11.9	10.3	0.12	10.40	38
	WB7-6	3.15	7.1	130	0.14	2.033	1.935	14.3	12.2	0.21	5.91	47
	WB7-7	3.6	6.93	174	0.07	0.723	0.853	2.2	1.3	0.05	5.26	21
	WB7-8	4.05	5.94	332	0.20	0.060	0.031	<0.1	<0.2	0.01	3.78	133
	WB7-9	4.5	5.74	392	0.12	0.035	0.010	<0.1	<0.2	0.02	6.47	40
	WB7-12	5.85	5.36	440	0.11	0.027	nd	0.0	nd	0.01	4.29	53
	WB7-14	6.75	6.34	366	1.27	0.018	nd	0.7	<0.2	0.15	15.98	77
PZ6	WB7-34	0.9	6.37	347	8.74	0.093	0.075	0.4	<0.2	0.05	225.26	21
	WB7-35	1.2	6.38	336	7.33	0.207	0.248	0.5	<0.2	0.07	175.02	30
	WB7-36	1.5	6.7	324	5.35	0.070	0.091	0.1	<0.2	0.07	105.76	58
	WB7-37	2.1	7.63	157	0.37	1.385	1.300	2.4	<0.2	0.10	11.41	44
	WB7-38	2.4	7.47	158	0.18	0.554	0.462	0.4	<0.2	0.03	3.45	43
	WB7-39	2.7	7.1	243	0.27	0.328	0.332	<0.1	<0.2	0.02	12.02	61
	WB7-40	3	6.05	334	0.09	0.055	0.043	0.1	<0.2	0.02	4.23	111
	WB7-41	3.45	5.79	386	0.19	0.064	0.054	<0.1	<0.2	0.02	5.22	149
	WB7-42	3.9	5.76	396	0.14	0.018	0.023	<0.1	<0.2	0.01	2.56	62
PZ3	WB7-15	0.9	6.27	340	0.10	0.043	0.026	<0.1	<0.2	0.02	13.48	26
	WB7-16	1.35	5.89	353	0.07	0.077	0.065	<0.1	<0.2	0.02	6.59	42
	WB7-17	1.8	5.68	382	0.11	0.061	0.045	<0.1	<0.2	0.02	5.51	130
	WB7-18	2.25	5.74	371	0.12	0.063	0.003	<0.1	nd	0.02	4.18	87
	WB7-19	2.7	6.13	374	0.43	0.018	0.002	0.2	<0.2	0.05	10.47	17
	WB7-20	3	6.37	355	1.52	0.026	0.055	0.8	nd	0.12	45.38	13
	WB7-22	3.15	6.6	318	5.47	0.042	0.014	1.0	<0.2	0.28	106.40	29
	WB7-21	3.3	6.5	338	12.33	0.271	0.021	0.9	<0.2	0.36	272.78	473
	WB7-23	3.45	6.68	322	17.31	0.046	0.011	1.3	<0.2	0.42	431.80	908
	WB7-24	3.6	6.97	300	19.64	0.028	0.024	0.8	<0.2	0.40	450.74	1159
	WB7-25	3.75	7.21	282	20.73	0.029	0.024	1.6	<0.2	0.39	492.95	1694
	WB7-26	4.05	7.37	263	22.99	0.026	0.024	1.7	<0.2	0.37	539.80	2450
	WB7-27	4.5	7.45	271	24.85	0.257	0.002	0.2	<0.2	1.29	687.22	1876
	WB7-28	5.1	7.64	152	25.41	1.493	1.581	0.3	0.2	1.16	691.89	1384
	WB7-29	5.7	7.81	93	25.87	3.050	2.870	5.6	6.6	1.54	686.23	1268
	WB7-30	6.3	7.95	47	26.00	3.293	3.187	10.1	16.0	1.39	700.46	1317
	WB7-31	6.9	8.01	48	26.00	3.217	2.962	9.8	10.3	1.04	690.73	874
	WB7-32	7.5	8.02	44	26.00	3.691	3.501	9.6	11.3	2.63	724.28	586
	WB7-33	8.1	8.02	26	26.00	3.996	3.910	12.3	16.0	1.40	690.76	397

*nd: not determined; Total dissolved As concentration in bay water = 0.3 μg L^{-1}.

Table S2. Sediment Chemistry Data

Piezometer No	Sample No	Depth	1.2N HCl leaching						1M P extraction	
			FeII/Fe	Fe	P	S	Mn	As	As	AsIII
		m		mg/kg	mg/kg	mg/kg	mg/kg	ug/kg	ug/kg	ug/kg
PZ7	H2-1	0.2	0.22	1040	57.21	18.63	27.65	208	247	
N = 6	H2-2	0.3	0.24	759	41.05	24.97	48.41	213	230	
	H2-3	0.5	0.21	587	44.15	25.52	16.87	286	301	
	H2-4	1.3	0.74	463	42.17	23.05	3.08	140	54	
	H2-5	1.9	0.91	536	79.31	29.45	5.60	115	55	
	H2-6	2.4	0.84	464	87.10	18.21	7.22	150	51	
PZ6	H1-1	0.6	0.25	730	203.89	63.29	3.24	387	197	<0.1
N = 13	H1-2	1.0	0.44	375	130.21	18.55	2.96	190	109	
	H1-3	1.1	0.46	354	77.19	10.02	2.85	129	80	<0.1
	H1-4	1.7	0.69	229	46.75	8.23	2.56	70	49	
	H1-6	1.8	0.93	211	33.44	8.59	2.21	107	28	1.5
	H1-5	2.1	0.71	286	37.18	10.71	2.34	114	43	4.7
	H1-7	2.1	0.68	404	38.81	13.34	3.40	151	65	4.1
	H1-8	2.6	0.70	271	36.27	10.60	1.80	155	104	3.2
	H1-9	2.9	0.46	437	24.95	13.98	1.99	92	127	1.0
	H1-10	3.2	0.27	354	18.11	7.61	1.41	48	122	
	H1-11	3.5	0.36	252	17.46	6.59	1.75	72	230	0.3
	H1-12	3.8	0.18	457	16.39	6.12	1.86	100	246	
	H1-13	4.2	0.20	420	12.45	7.08	2.06	98	202	0.6
PZ11*	PZ11-1	0.5		840				151	<30	
N = 18	PZ11-2	0.8		764				<30	<30	
	PZ11-3	1.1		1264				<30	<30	
	PZ11-4	1.6		772				61	<30	
	PZ11-5	1.9		624				63	<30	
	PZ11-6	2.4		1306				147	<30	
	PZ11-7	3.1		879				62	<30	
	PZ11-8	3.5		653				88	<30	
	PZ11-9	3.7		621				78	<30	
	PZ11-10	3.8		740				183	75	
	PZ11-11	4.2		718				124	101	
	PZ11-12	4.4		580				61	165	
	PZ11-13	4.8		1356				70	<30	
	PZ11-14	5.0		1637				73	<30	
	PZ11-15	5.3		1426				719	451	
	PZ11-16	5.6		1417				245	393	
	PZ11-17	5.9		898				597	315	
	PZ11-18	6.2		702				351	222	
PZ3	H3-1	0.1	0.27	237	13.29	86.55	3.00	114	135	
N = 7	H3-2	0.3	0.32	544	20.24	29.24	6.10	115	146	
	H3-3	0.5	0.10	987	42.80	19.93	5.89	378	389	
	H3-4	0.8	0.11	749	46.51	15.06	2.58	400	436	
	H3-6	1.1	0.12	781	41.68	11.34	2.05	340	426	
	H3-5	1.5	0.07	1081	38.76	7.97	2.46	351	531	
	H3-7	2.1	0.08	488	15.97	6.87	2.13	94	272	

*PZ11 has no FeII/Fe data reported because it was not determined immediately after sampling.

Table S3. As speciation and concentration in supernatant and sediment of sorption experiment

Sample No	Initially added AsIII	As in supernatant after 1 week	As in supernatant after 2 weeks	Sorbed As	Estimated sorbed As by Langmuir isotherm	P-ext AsIII	P-ext AsV	HCl-ext AsT	Sorption Capacity	K_{La}	Kd
	ug/L	ug/L	ug/L	ug/kg	ug/kg	ug/kg	ug/kg	ug/kg	ug/kg	L/ug	L/kg
PZ7									1520	0.038	30
2-4E5	622	10	8	367	361	26	298	145			
2-4E10	1176	19	20	566	656	32	328	171			
2-4E15	1866	37	33	1057	842	43	552	226			
2-4E20	2308	68	63	1019	1065	67	610	317			
PZ6									1750	0.067	42
1-1E5	940	8	7	578	582	5	385	219			
1-1E10	1880	21	18	1095	973	5	615	294			
1-1E15	1883	26	24	990	1082	5	772	326			
1-1E20	2254	23	20	995	1004	28	749	362			
PZ3									4760	0.029	83
3-6E5	653	23	3	403	403	17	619	237			
3-6E15	1847	24	8	934	927	75	856	375			
3-6E20	2537	53	15	1403	1412	81	1091	383			

*Sorption capacity of 1100 ug/kg for PZ7 sediment is determined from sorption experimental data

#Sorbed As calculated by mass balance uses As concentration in supernatant after 2 weeks.

Table S4. Surface Complexation Reactions and equilibrium constants (log K) used in Geochemical Modeling of As(III) Sorption Isotherms (Dzombak and Morel, 1990)

Surface reaction	Equilibrium constant (log K) DLM-HFO/SCM
$SOH = SO^- + H^+$	-8.93
$SOH + H^+ = SOH^{2+}$	7.29
$SOH + H_3AsO_3 = SH_2AsO_3 + H_2O$	5.41
$SOH + H_3AsO_4 = SH_2AsO_4 + H_2O$	8.61
$SOH + H_3AsO_4 = SHAsO_4^- + H_2O + H^+$	2.81
$SOH + H_3AsO_4 = SOHAsO_4^{3-} + 3H^+$	-10.12

Table S5. Summary of distribution coefficients (Kd) of As for variable types of soil and sediment from field investigation and laboratory experiment

| Method	References	Type of sample	Kd (L/kg)
Field investigation	Baes and Sharp (1983; J of Environ Qual)	Agricultural soils and clay	6.7 (1.9-18) for As(V)
	Sullivan and Aller (1996; Geochim Cosmochim Acta)	Sediment from Amazon Shelf	11~5000
	Manning and Goldberg (1997, Soil Sci)	Californian soils	5~521 for As(III), 10~80 for As(V)
	DPHE/BGS/MML (1999)	Bangladesh sediment	~1 under high P-low Fe
			> 200 under low P-high Fe conditions
	BGS & DPHE (2001)	Bangladesh sediment	2~6
	van geen et al (2008, Environ Sci Technol)	Bangladesh sediment	~4
Laboratory experiment	Kuhlmeier (1997, J of Soil Contam)	Highly contaminated clayey and sandy soils	0.26~3.3
	Williams et al (2003, J of Environ Qual)	Soils from the Melton Brach watershed	345
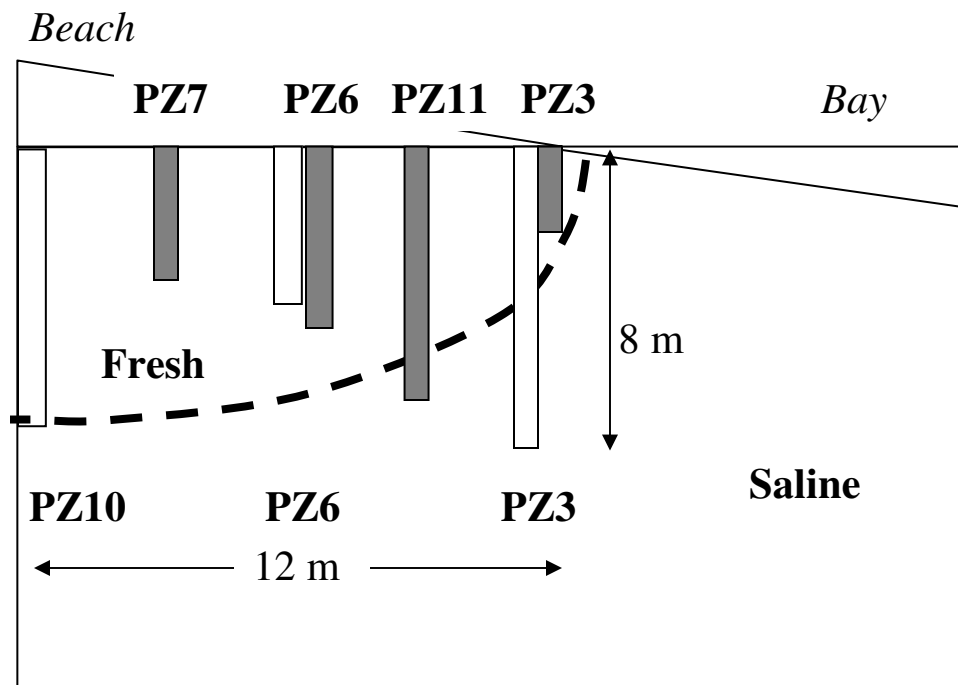
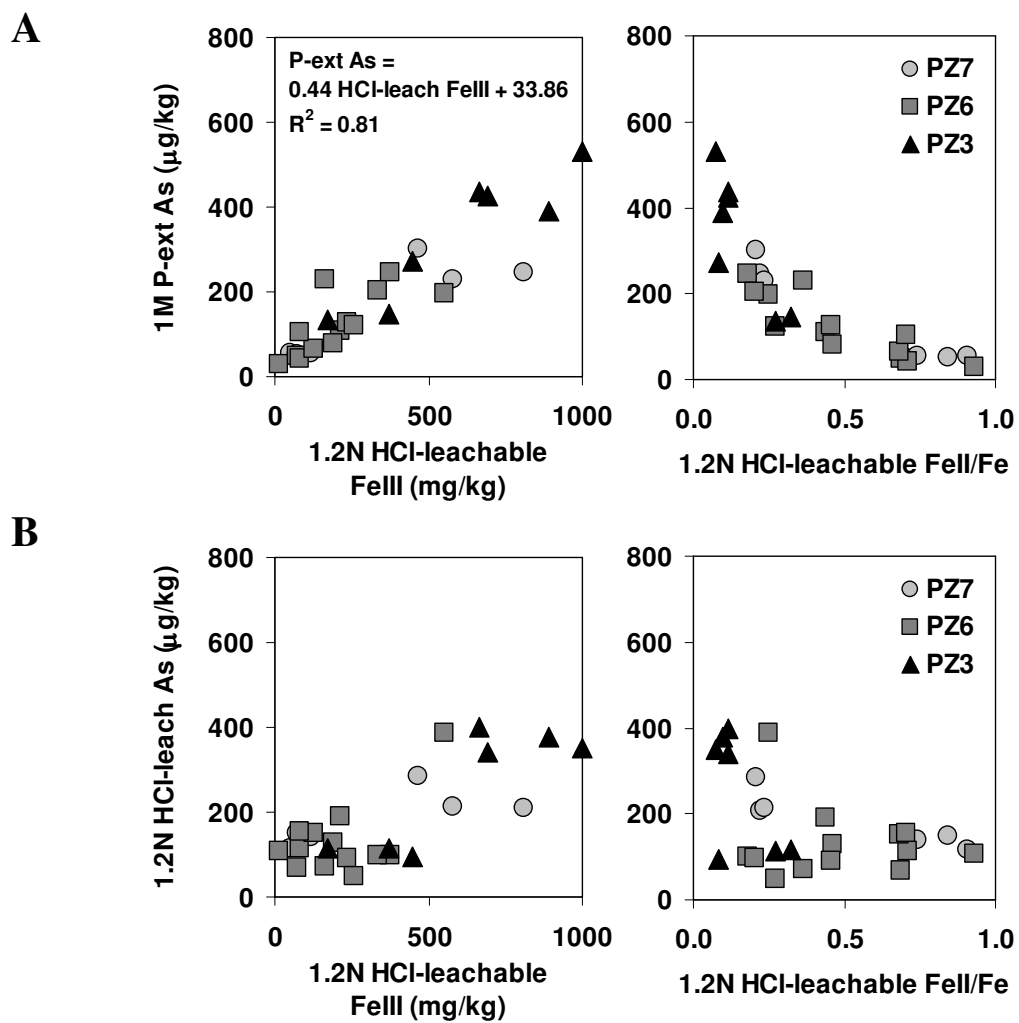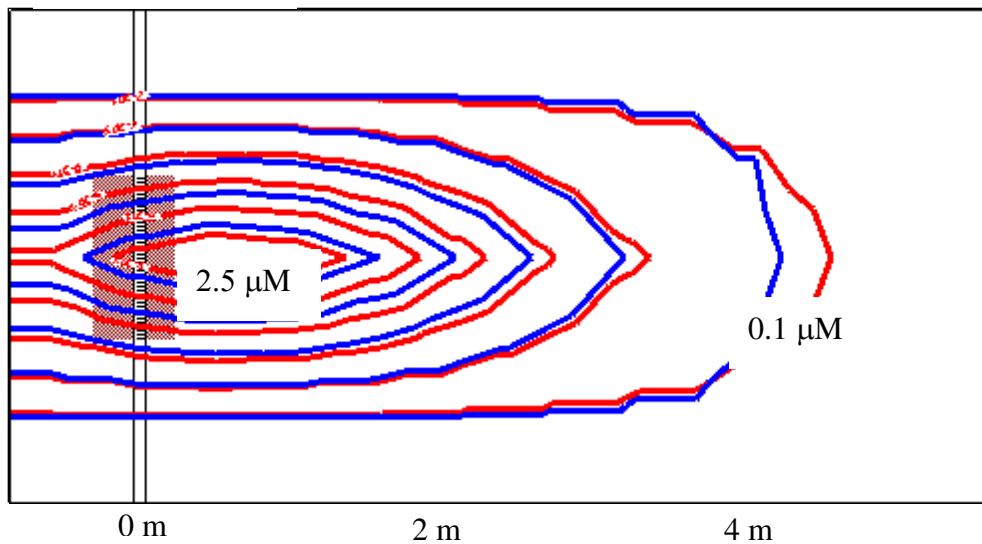**Figure S1**. Location of pore water (white bar) and sediment core (gray bar) transect.

Figure S2. A. Correlation between 1M P-extractable As and sedimentary Fe(III) or Fe(II)/Fe; B. Correlation between 1.2N HCl-leachable As and sedimentary Fe(III) or Fe(II)/Fe.

Injection well

2.5 μM

0.1 μM

0 m   2 m   4 m

Hydraulic properties	Hydraulic Cond (Kx,y)	86.4 m/d
	hydraulic gradient	0.0015
	Effective porosity	0.39
Initial GW chemistry	FeII	20 uM
	DO	0 uM
	pH	6.5
Injection well	period	4 weeks
	AsV	6.7 uM
	AsIII	0
	NO3	100 uM
	DO	20 uM
	FeII	0 uM
Sewage plume	FeII	500 uM
	pH	6.5
	AsIII	0.15 uM
	AsV	0.02
	DO	0 uM
	NO3	0 uM

Figure S3. PHT3D simulation result for As(III) (red) and As(V) (blue) plumes in 100 days after starting of As (V) injection by applying Kd of 4 L/kg, which is based on Höhn et al (2006)' s As(V) injection experiment. The table summarizes the hydraulic properties and chemistry of groundwater applied for PHT3D modeling.
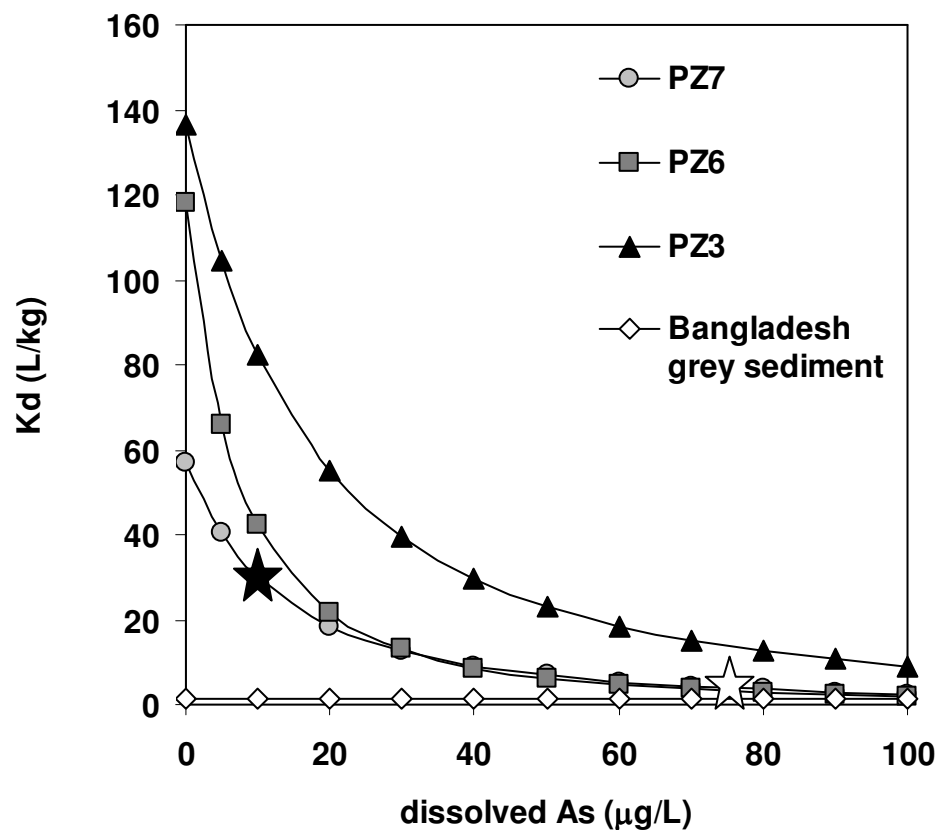
Figure S4. Variation of distribution coefficient (Kd) as a function of dissolved As at equilibrium for sediments from PZ7, PZ6, and PZ3. Solid star represents our study area, which corresponds to dissolved As of 10 μg/L and Kd of 30 L/kg, while open star represents Höhn et al (2006)'s As(V) injection experiment, in which dissolved As concentration in the plume was on average ~75 μg/L, resulting in Kd of 4 L/kg. Line with diamond symbols represents grey sediment from Bangladesh aquifer, which has K_{La} of 0.00038 L/μg and As sorption capacity of 3380 μg/kg (Jung, unpublished).